❐   674

Robust control of wind turbine based on doubly-fed induction generator optimized by genetic algorithm

Noureddine Elmouhi[1,2], Ahmed Essadki[1], Hind Elaimani[1,2]
[1]Research Center of Engineering and Health Sciences and Technologies (STIS), Ecole Nationale Supérieure d'Arts et Métiers (ENSAM), Mohammed V University in Rabat, Rabat, Morocco
[2]Laboratory of Innovation in Management and Engineering for Enterprise, Institut supérieur d'ingénierie et des affaires (ISGA Rabat), Rabat, Morocco

ABSTRACT

In this research paper we will cover the study of the modelling and the control methods of the variable speed wind turbine based on doubly-fed induction generator (DFIG). It represents the most stressed structure given its distinctive characteristics. To control the electrical powers generated by this system independently, the vector control with the stator flux orientation is founded according to two techniques: i) the control of the powers by the backstepping technique and ii) the robust control based on the active disturbances rejection control. After the synthesis of the controllers of those two methods, their performances will be tested and compared to evaluate their effectiveness. We are mainly interested in the robustness test of the two control strategies with respect to the internal parameters' fluctuation of the generator. The computing of the different parameters regulators of these two strategies is carried out using a genetic algorithm. This computing method makes it possible to arrive at an optimal solution of the DFIG power control. The different parts are simulated using MATLAB/Simulink environment.

This is an open access article under the CC BY-SA license.

Corresponding Author:

Noureddine Elmouhi
Research Center of Engineering and Health Sciences and Technologies (STIS)
Ecole Nationale Supérieure d'Arts et Métiers (ENSAM), Mohammed V University
Angle Avenue Allal El Fassi et, Rue Al Mfaddal Cherkaoui, Rabat, Morocco
Email: n.elmouhi@gmail.com

NOMENCLATURE

R	: Turbine radius	f	: Coefficient of viscous friction
P	: Air density	G	: Gain multiplier
v	: Wind speed	Φ_{sdq}	: dq axis Stator fluxes
Ω_t	: Turbine speed	Φ_{rdq}	: dq axis Rotor fluxes
C_p	: Power coefficient	V_{sdq}	: Stator voltages according to dq axis
λ	: Velocity ratio	V_{rdq}	: Rotor voltages according to dq axis
β	: Pich angle	i_{sdq}	: Stator currents according to dq axis
J	: Total inertia	i_{rdq}	: Rotor currents according to dq axis
$J_{Turbine}$	: Turbine inertia	ω_s	: Rotor angular frequency
J_g	: Generator inertia	ω_r	: Stator angular frequency

1. INTRODUCTION

Faced with the ever-increasing demand for energy, industrialized countries have made massive use of nuclear power plants. This type of energy has the advantage of not causing atmospheric pollution, but the risk of nuclear accident [1], [2]. Nowadays countries are increasingly turning to the use of renewable energy sources as a solution to that problem. Wind power in term of example, which represent an attractive alternative that may in the future replace traditional power plants [1], [3], [4].

The variable speed wind turbine based on a doubly-fed induction generator (DFIG), driven by a turbine and controlled by the rotor is the most used system in wind energy conversion considering the advantages it offers [3], [5]-[7]. In this structure, the stator of the generator is connected directly to the grid, on the other hand the rotor is linked to the grid via a transformer and link filter with two bidirectional converters [3], [4], [8], [9]. Figure 1 shows the functional scheme of this structure based on the DFIG and two power converters.

For this system command, various approaches are available in the literature. A study by Nadour and Essadki [10] shows that the backstepping approach provides good results compared to the proportional integral (PI) control especially with regard to the hounding the references values and robustness against external and internal disturbances. However, this approach does not present more significant results faced with the change of internal DFIG parameters with higher variation rates (100% for example). Especially since it does not present an analytical method allowing the computing of the regulator parameters.
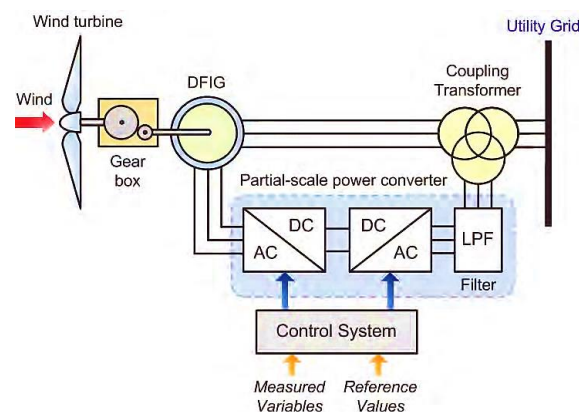

Figure 1. Wind turbine structure based on DFIG [1]

Bossoufi and Karim [11] have presented a control technique based on a control approach of pole placement incorporated with a backstepping control system. The experimental results obtained based on a prototyping platform realized with DFIG-generator, field programmable gate array (FPGA) and wind turbine [11] show the efficiency of the technique for the system stability. The problem of this solution is that it does not present any detail about the robustness in the case of internal parameters' variation. Indeed, these parameters may undergo changes caused by many physical phenomena (temperature, inductors saturation) [12].

Rouabhi and Rachid [13] presented a combination of vector and backstepping control. Simulation results show the decoupled control of both electrical powers and a good performance likened to the results acquired in the case of the compensator use. However, we do not find in this approach a method for the synthesis of the controllers' parameters, on which the performances of this approach are based.

To ensure system stability and rapid dynamic response, the control parameters must be well chosen. However, in all the previous works and in the majority of the documents which treat the same subject, one does not find a study which presents a procedure for the determination of these control strategy parameters. The calculation is often done by a random adjustment during the simulation.

In recent years, several works have dealt with the DFIG command used in wind energy conversion system (WECS) by active disturbance rejection control (ADRC) [14]-[16]. With this control method, the system is able to compensate external disturbances and those due to parameter changes. The work of this research paper is focused on the study and comparison of this methods robustness with that based on backstepping. We also propose a method based on genetic algorithms, for the calculation of the different controllers' parameters, which allows to arrive at an optimal solution of DFIG power control. We can show that replacing backstepping controllers with ADRC controllers optimized by genetic algorithm (GA) allows to improve significantly the system performances.

This paper is structured as shown in: the first part is devoted to the studied system modeling with its different components. In the next part, we treat the DFIG control principle by the backstepping technique. The third part is entirely devoted to the presentation of the DFIG robust control founded on the ADRC. The next part is devoted to the presentation of the procedure used for the optimization of the two control approaches using the genetic algorithm. The last section of this paper is devoted to the presentation and analysis of the simulation results, and the robustness test using the MATLAB/Simulink environment.

2. RESEARCH METHOD
2.1. Modelling of wind turbine using DFIG
2.1.1. Wind turbine model
The wind turbine converts the kinetic wind energy and drives the variable speed generator. The maximum power which can be obtained according to Betz's law is [17]-[19]:

$$P_{extr} = \frac{1}{2}\rho \pi R^2 v^3 C_p(\beta, \lambda) \tag{1}$$

where C_p is the power coefficient, which is defined by the ratio between the total extracted power and the incident one [17]. This coefficient depends on λ, the velocity ratio, and β the pich angle, it is formulated by the following function [16], [20]:

$$C_p(\lambda, \beta) = \frac{1}{2}\left(116(\frac{1}{\lambda+0.08\beta} + \frac{0.035}{1+\beta^3}) - 0.4\beta - 5\right)e^{-21(\frac{1}{\lambda+0.08\beta}+\frac{0.035}{1+\beta^3})} + 0.0068\lambda \tag{2}$$

the aerodynamic torque T_{aer} is given by:

$$T_{aer} = \frac{P_{extr}}{\Omega_t} = \frac{1}{2.\Omega_t}\rho \pi R^2 v^3 C_p(\beta, \lambda) \tag{3}$$

$$J\frac{d\Omega_{mec}}{dt} + f\Omega_{mec} = T_g - T_{em} \tag{4}$$

$$J = \frac{J_{Turbine}}{G^2} + J_g \tag{5}$$

from (1), (3), and (5), we can deduce the functional diagram of the turbine model which is illustrated in this Figure 2.
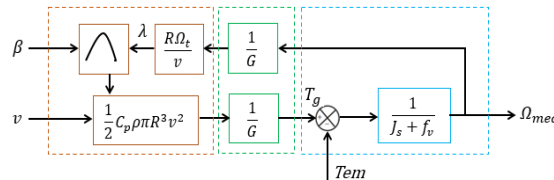

Figure 2. Functional scheme of turbine model

2.1.2. DFIG modelling
The equations which describe the electric part of the generator in the two-phase reference are given by the following relations [12], [21]:

$$\begin{cases} \varphi_{sd} = L_s I_{sd} + L_m I_{rd} \\ \varphi_{sq} = L_s I_{sq} + L_m I_{rq} \\ \varphi_{rd} = L_r I_{rd} + L_m I_{sd} \\ \varphi_{rq} = L_r I_{rq} + L_m I_{sq} \end{cases} \tag{6}$$

$$\begin{cases} V_{sd} = R_s I_{sd} + \frac{d\varphi_{sd}}{dt} - \omega_s\varphi_{sq} \\ V_{sq} = R_s I_{sq} + \frac{d\varphi_{sq}}{dt} + \omega_s\varphi_{sd} \\ V_{rd} = R_r I_{rd} + \frac{d\varphi_{rd}}{dt} - \omega_r\varphi_{rq} \\ V_{rq} = R_r I_{rq} + \frac{d\varphi_{rq}}{dt} + \omega_r\varphi_{rd} \end{cases} \tag{7}$$

the equation describing the mechanical part is as shown in [21]:

$$T_{em} = p\frac{L_m}{L_s}(I_{rd}\varphi_{sq} - I_{rq}\varphi_{sd} \tag{8}$$

where p=2 is the number of pole pairs. We have considered the stator flux control oriented along the d axis of the two-phase reference. It is also considered that the stator resistance Rs is negligible during the model computing [12], [17], [21], [22]. So, we deduce:

$$\begin{cases} \varphi_{sd} = \varphi_s = cte \\ \varphi_{sq} = 0 \end{cases} \tag{9}$$

$$\begin{cases} V_{sd} = 0 \\ V_{sq} = V_s = \omega_s\varphi_s \\ V_{rd} = R_rI_{rd} + \frac{d\varphi_{rd}}{dt} - \omega_r\varphi_{rq} \\ V_{rq} = R_rI_{rq} + \frac{d\varphi_{rq}}{dt} + \omega_r\varphi_{rd} \end{cases} \tag{10}$$

$$\begin{cases} \varphi_{sd} = \varphi_s = L_sI_{sd} + L_mI_{rd} \\ 0 = L_sI_{sq} + L_mI_{rq} \\ \varphi_{rd} = L_rI_{rd} + L_mI_{sd} \\ \varphi_{rq} = L_rI_{rq} + L_mI_{sq} \end{cases} \tag{11}$$

$$\begin{cases} I_{sd} = \frac{\varphi_s}{L_s} - \frac{L_m}{L_s}I_{rd} \\ I_{sq} = -\frac{L_m}{L_s}I_{rq} \end{cases} \tag{12}$$

$$T_{em} = -\frac{3}{2}p\frac{L_mV_s}{L_s\omega_s}I_{rq} \tag{13}$$

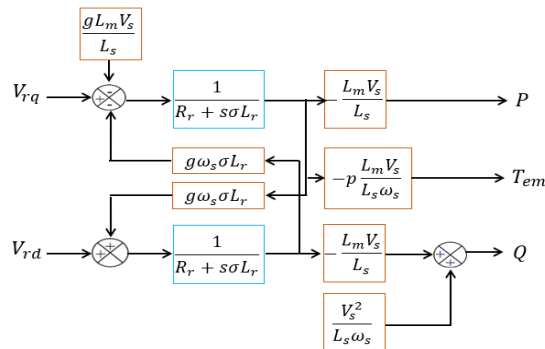Finally, we can deduce the block diagram of the DFIG model (Figure 3).

Figure 3. Block diagram of the DFIG model

2.2. Powers control using the backstepping technique
2.2.1. Backstepping principle

The principle of backstepping relies on its ability to dissociate a complex nonlinear problem control for a system into simpler ones. Basically, this technique synthesis is separated into different design steps. At each one, we're virtually dealing with a simpler system with single-input and single-output problem, and each sub system supply a baseline for the next synthesis step. The global stability and overall performance are obtained by a Lyapunov function for the global system [4], [6], [11], [13].

2.2.2. DFIG control based on the backstepping method

The backstepping method that we are going to apply for controlling the double-fed asynchronous machine is based on the vector control. In this approach, the command will be established in the reference (d and q) according the condition in (11). The control of the rotor side converter (RSC) allows the regulation of

the exchanged powers with the grid. the synthesis of the control blocks with the backstepping method is divided into two subsystems: the first one is to generate the current reference I_{rd} and I_{rq} and the second one is to generate the voltage reference V_{rd} and V_{rq} [4], [10], [23]. the relations linking the stator powers and the rotor currents are expressed by (14) and (15):

$$\begin{cases} P_S^{ref} = -\frac{V_S.L_m}{L_S}.I_{rq}^{ref} \\ Q_S^{ref} = \frac{V_S^2}{w_S.L_S} - \frac{V_S.L_m}{L_S}.I_{rd}^{ref} \end{cases} \tag{14}$$

$$\begin{cases} I_{rq}^{\dot{ref}} = -\frac{L_S}{V_S.L_m}.P_S^{\dot{ref}} \\ I_{rd}^{\dot{ref}} = -\frac{L_S}{V_S.L_m}.Q_S^{\dot{ref}} \end{cases} \tag{15}$$

the rotor currents derivatives can be mathematically determined and given by the following:

$$\frac{dI_{rd}}{dt} = \left(V_{rd} - R_r.I_{rd} + g.w_s.L_r.\sigma.L_{rq}\right).\frac{1}{L_r.\sigma} \tag{16}$$

$$\frac{dI_{rq}}{dt} = \left(V_{rq} - R_r.I_{rq} - g.w_s.L_r.\sigma.L_{rd} - g.w_s.\frac{L_m.V_s}{w_s.L_s}\right).\frac{1}{L_r.\sigma} \tag{17}$$

where $\sigma = (1 - \frac{L_m^2}{L_s L_r})$ represent the dispersion coefficient. The computing of the reference quantities of the currents and voltages control is based on the Lyapunov functions according to two steps [4], [11]-[13].

- Step 1: the errors E_1 and E_2 between the currents I_{rq}, I_{rd} and their reference I_{rqref} and I_{rdref} is given by (18).

$$\begin{cases} E_1 = I_{rq}^{ref} - I_{rq} \\ E_2 = I_{rd}^{ref} - I_{rd} \end{cases} \tag{18}$$

The derivative of this error is given by (19).

$$\begin{cases} \dot{E}_1 = I_{rq}^{\dot{ref}} - \dot{I}_{rq} \\ \dot{E}_2 = I_{rd}^{\dot{ref}} - \dot{I}_{rd} \end{cases} \tag{19}$$

We select the Lyapunov function so such that:

$$v = \frac{1}{2}(E_1^2 + E_2^2) \tag{20}$$

The errors are chosen so as to have a zero derivative of the Lyapunov function:

$$\dot{E}_1 = -K_1 E_1 \text{ where: } K_1 > 0 \tag{21}$$

$$\dot{E}_2 = -K_2 E_2 \text{ where: } K_2 > 0 \tag{22}$$

$$v = -K_1 E_1^2 - K_2 E_2^2 \tag{23}$$

$$\dot{E}_1 = \left(-\frac{L_S}{V_S.L_m}.\dot{P}_S^{ref}\right) - \frac{1}{L_r.\sigma}\left(V_{rq} - R_r.I_{rq} - g.w_s.L_r.\sigma.I_{rd} - g.\frac{L_m.V_S}{L_S}\right) \tag{24}$$

$$\dot{E}_2 = \left(-\frac{L_S}{V_S.L_m}.\dot{Q}_S^{ref}\right) - \frac{1}{L_r.\sigma}\left(V_{rd} - R_r.I_{rd} + g.w_s.L_r.\sigma.I_{rq}\right) \tag{25}$$

- Step 2:

$$-K_1 E_1 = \left(-\frac{L_S}{V_S.L_m}.\dot{P}_S^{ref}\right) - \frac{1}{L_r.\sigma}V_{rq} - \frac{1}{L_r.\sigma}\left(-R_r.I_{rq} - g.w_s.L_r.\sigma.I_{rd} - g.\frac{L_m.V_S}{L_S}\right) \tag{26}$$

$$-K_2 E_2 = \left(-\frac{L_S}{V_S.L_m}.\dot{Q}_S^{ref}\right) - \frac{1}{L_r.\sigma}V_{rd} - \frac{1}{L_r.\sigma}\left(-R_r.I_{rd} + g.w_s.L_r.\sigma.I_{rq}\right) \tag{27}$$

From the previous equations, the voltages reference can be mathematically determined:

$$V_{rq} = L_r.\sigma \left(-\frac{L_s}{V_s.Lm}.\dot{P}_s^{ref} + K_1 E_1\right) + R_r.I_{rq} + g.w_s.L_r.\sigma.I_{rd} + g.\frac{Lm.V_s}{Ls} \tag{28}$$

$$V_{rd} = L_r.\sigma \left(-\frac{L_s}{V_s.Lm}.\dot{Q}_s^{ref} + K_2 E_2\right) + R_r.I_{rd} + g.w_s.L_r.\sigma.I_{rq} \tag{29}$$

K_1 and K_2 are the backstepping controller parameters, they are strictly positive, and ensure the system stability as well as a fast dynamic response [14]. These performances are ensured with a zero derivative of Lyaponov function. The functional scheme of the backstepping command is given in the Figure 4.
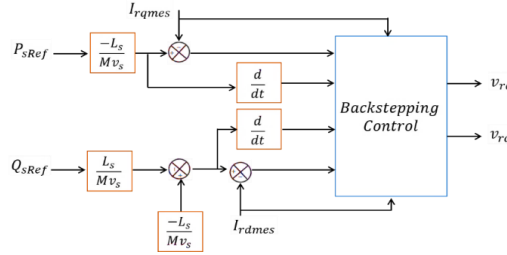
Figure 4. Block diagram of the control structure by backstepping

2.3. Active disturbance rejection control strategy

The ADRC is a robust control strategy which is based on the model system extension using a state observer extended state observer (E.S.O) to have an estimation and to cancels, in real time, all disturbances affecting the system whether internal or external [15], [16], [18], [24]-[26]. To explain the principle of the ADRC, we treat the case of a first order system:

$$\frac{dy(t)}{dt} = -\frac{1}{T}y(t) + b.u(t) \text{ where: } b = b_0 + \Delta b \text{ and } b_0 = \frac{K}{T} \tag{30}$$

where b is a parameter to be estimated, b_0 represents the known part of b and Δb represents the modeling error due to the system parameters changes. *u* and *y* are input and output variables, K is the static gain and T is a system constant.

$$\begin{cases} \dfrac{dy(t)}{dt} = -\dfrac{1}{T}y(t) + \Delta b.u(t) + b_0.u(t) \\ \dfrac{dy(t)}{dt} = f(y,d,t) + b_0.u(t) \end{cases}$$

where:

$$f(y,d,t) = -\frac{1}{T}y(t) + \frac{1}{T}d(t) + \Delta b.u(t)\frac{1}{T}y(t) \tag{31}$$

f(y,d,t) represents the effect resulting from internal parameters variations and the external disturbances impact. The basic idea is the estimation and compensation of the disturbance. The (31) can be written in an augmented state space form as [27]:

$$\begin{cases} \dot{x_1} = x_2 + b_0.u \\ \dot{x}_2 = h \\ y = x_1 \end{cases}$$

where $h = \dot{f}$ \hfill (32)

$$\begin{cases} \dot{x} = Ax + b_0 Bu + Eh \\ y = Cx \end{cases} \tag{33}$$

where: $A = \begin{pmatrix} 0 & 0 \\ 0 & 0 \end{pmatrix}$, $B = \begin{pmatrix} b_0 \\ 0 \end{pmatrix}$, $C = (1\,0)$ and $E = \begin{pmatrix} 0 \\ 1 \end{pmatrix}$. The observer will be able to estimate the derivatives of y and f and it is developed as shown in:

$$\begin{cases} \dot{x} = Ax + b_0 Bu + L(y - \tilde{y}) \\ \tilde{y} = Cx \end{cases} \tag{34}$$

where L represent the observer's gain vector.

$$L = \begin{pmatrix} \beta_1 \\ \beta_2 \end{pmatrix}$$

In Figure 5(a), we represent the structure of the ADRC controller previously studied [14], [15], and the structure of the extended state observer is given by the Figure 5(b) [28].
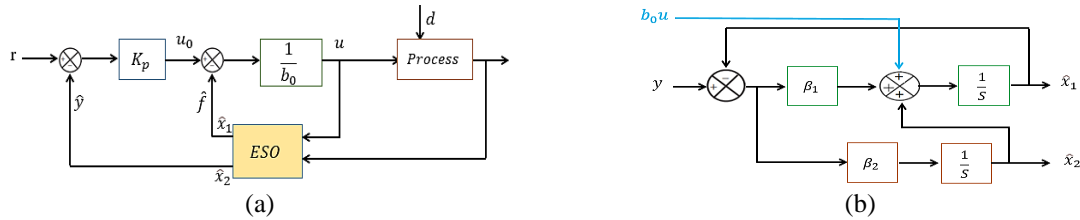

(a)   (b)

Figure 5. Structure of (a) the ADRC controller and (b) ESO

a) Control of the rotor side converter

By referring to the assumptions relating to the stator flux orientation along the d-axis, and neglecting the stator resistance, the equations of the mathematical model of DFIG can be simplified [16]. So, the rotor currents are expressed by the following relations:

$$\frac{di_{rd}}{dt} = -\frac{R_r}{\sigma L_r} i_{rd} + \omega_r . i_{rq} + \frac{1}{\sigma L_r} V_{rd} \tag{35}$$

$$\frac{di_{rq}}{dt} = -\frac{R_r}{\sigma L_r} i_{rq} - \omega_r . i_{rd} - \omega_r \frac{L_m}{\sigma L_r L_s} \Phi_s + \frac{1}{\sigma L_r} V_{rq} \tag{36}$$

we can also put these relations in the (37) and (38).

$$\frac{di_{rd}}{dt} = f_d(i_{rd}, d, t) + b_{r0} u(t) \text{ where: } \begin{cases} f_d = -\frac{R_r}{\sigma L_r} i_{rd} + \omega_r . i_{rq} + (\frac{1}{\sigma L_r} - b_0) V_{rd} \\ u = V_{rd} \ , \ b_0 = \frac{1}{\sigma L_r} \end{cases} \tag{37}$$

$$\frac{di_{rq}}{dt} = f_q(i_{rq}, d, t) + b_{r0} u(t) \text{ where: } \begin{cases} f_q = -\frac{R_r}{\sigma L_r} i_{rq} - \omega_r . i_{rd} - \omega_r \frac{L_m}{\sigma L_r L_s} \Phi_s + (\frac{1}{\sigma L_r} - b_0) V_{rq} \\ u = V_{rq} \ , \ b_{r0} = \frac{1}{\sigma L_r} \end{cases} \tag{38}$$

f_d and f_q represent the disturbances impacting the rotor currents I_{rd} and I_{rq}. V_{rd} and V_{rq} are respectively the command variables of the current's loops I_{rd} and I_{rq}. b_{r0} represent the known part of the process parameters. The schematic diagram of the rotor side control is given by Figure 6. The parameters K_p, β_1 and β_2 are determined to have a perfect follow-up of I_{dr} and I_{qr} references values. These parameters are obtained in our case using GA.

b) Control of the GSC

The currents i_{qf} and i_{df} are given by (39).

$$\frac{di_{df}}{dt} = \frac{1}{L_f} V_{sd} - \frac{R_f}{L_f} i_{df} - w_s i_{qf} - \frac{1}{L_f} V_{df} \tag{39}$$

$$\frac{di_{qf}}{dt} = \frac{1}{L_f} V_{sq} - \frac{R_f}{L_f} i_{qf} - w_s i_{df} - \frac{1}{L_f} V_{qf} \tag{40}$$

The previous relations can be put in the (41) and (42).

$$\frac{di_{df}}{dt} = f_{df}(i_{df}, d, t) + b_0 u(t) \text{ where: } \begin{cases} f_{df} = \frac{1}{L_f} V_{sd} - \frac{R_f}{L_f} i_{df} - w_s i_{qf} + (\frac{1}{L_f} - b_0) V_{df} \\ u = V_{df} \ , \ b_{f0} = -\frac{1}{L_f} \end{cases} \tag{41}$$

$$\frac{di_{qf}}{dt} = f_{qf}(i_{qf}, d, t) + b_0 u(t) \text{ where: } \begin{cases} f_{qf} = \frac{1}{L_f}V_{sq} - \frac{R_f}{L_f}i_{qf} - w_s i_{df} + (\frac{1}{L_f} - b_0)V_{qf} \\ u = V_{qf}, \ b_{f0} = -\frac{1}{L_f} \end{cases} \quad (42)$$

The computing of the parameters used in the regulation algorithm, is done to have a perfect tracking of the reference values by the currents i_{qf} and i_{df}. This control algorithm by ADRC can be summarized according to Figure 7.
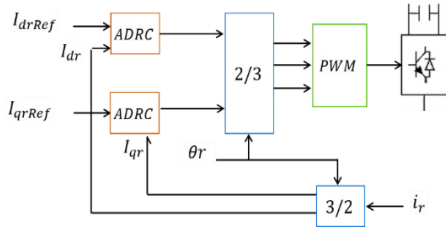

Figure 6. The GSC control diagram using ADRC   Figure 7. The GSC control diagram using ADRC
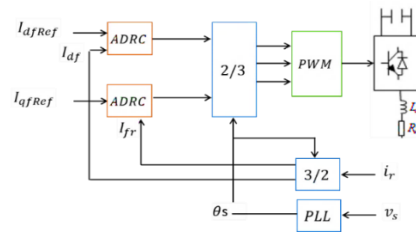
2.4. Genetic algorithm

The genetic algorithm is an optimization method for finding optimal solutions to research problems. It is based on the natural selection methods. This approach was proposed by John Holland in 1975, and then adopted as a very efficient method to find the solutions to an optimization problem. It makes it possible to avoid the local minima constituting a major problem in the case of nonlinear systems [29], [30].

The basic principle is based on the repeated modification of the population so as to evolve towards an optimal solution, and this starting from an initial population consisting of a certain number of elements appointed chromosomes. The relevance of each solution is measured by a fitness function. The algorithm is based primarily on three stages: selection, crossing, and mutation. These three operations must be applied to create new individuals to be evaluated with respect to their parents. The algorithm stops when we obtain individuals with optimal performances [29], [31], [32].

In the case of DFIG powers' control, the objective function can be computed and evaluated for each individual belonging to the actual population. Therefore, the parameters of the ADRC or backstepping controller can be decoded for each individual, then the DFIG model is simulated to obtain the objective function value which consists in following the reference power required by the turbine. The following population is generated based on the genetic algorithm operators (selection, crossing and mutation) [30], [33]. These two steps are repeated from generation to generation until a final population is obtained. In Figure 8, we present the optimization diagram to be carried out to reach the optimal parameters values of the backstepping and ADRC regulators. The types of the GA operations used and the parameters' initialization are given in Tables 1 and 2. In this work, the power of the machine used is 1.5 MW. The algorithm stops when the best fitness value is less than or equal to the limit fitness value which has been set here at 5.10^{-4} MW.
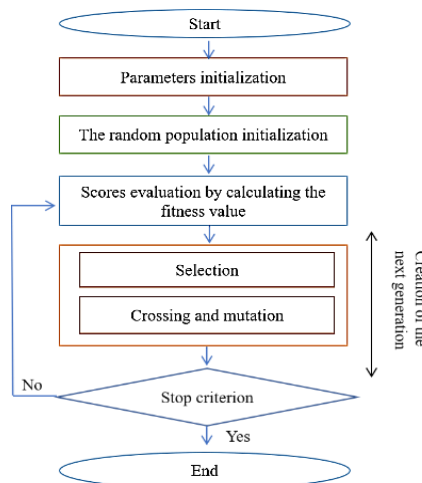

Figure 8. Optimization block diagram based on genetic algorithm

Table 1. Types of the GA operations used

Property	Type
Selection	GA default selection function
Mutation	Uniform
Crossover	Arithmetic

Table 2. Genetic algorithm parameters

Property	Value	
	Backstepping	ADRC
Variables to optimize	2	3
Population size	50	50
Maximum size of generations	500	500
Mutation fraction	0.01	0.01
Crossover fraction	0.08	0.08
Tolerance	5.10^2	5.10^2

2.4.1. Parameter's optimisation using GA for backstepping technique

As mentioned before, the control system must be able to guarantee the two main objectives: closed loop stability of the system and zero regulation of the tracking error. The problem which arises at this level is the determination of the backstepping adjustment coefficients K_1 and K_2. To avoid determining the gains of the regulators with non-analytical methods (random), we propose in this work an optimization by the genetic algorithm. The principle consists in considering an adaptation law established by the Lyapunov function as a minimization problem. This function is given as presented before by (43) [10], [11], [13].

$$v = -K_1 E_1^2 - K_2 E_2^2 \tag{43}$$

Where $E_1 = I_{rq}^{ref} - I_{rq}$ and $E_2 = I_{rd}^{ref} - I_{rd}$. In fact, the control of the I_{rq} and I_{rd} currents allows the generation of an active power P in accordance with the reference power required by the mechanical part (turbine). A GA based backstepping control optimization can be represented as shown in Figure 9.
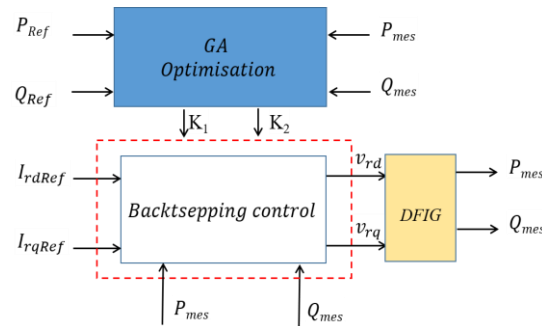

Figure 9. GA-based backstepping control optimization

2.4.2. Parameter's optimisation using GA for ADRC

The ADRC allows an estimation, using a state observer, of modeling uncertainties and external disturbances, and a compensation for them in real time [20]. The objective is to have a faster observer dynamic than the closed loop system one, as well as a reduced noise sensitivity [15], [16], [18], [28]. The genetic algorithm is used to determine the K_p, β_1 and β_2 parameters. These parameters are adjusted so as to obtain the optimum performance in terms of dynamics, robustness and disturbance's rejection. The objective function is therefore chosen to minimize the difference between the measured power and the reference one. A GA based ADRC optimization can be represented in Figure 10 and the parameters values used for genetic algorithm in this work are presented in Table 2.

$$P_S^{ref} = -\frac{V_S.L_m}{L_S}.I_{rq}^{ref} \tag{44}$$

$$Q_S^{ref} = \frac{V_S^2}{w_S.L_S} - \frac{V_S.L_m}{L_S}.I_{rd}^{ref} \tag{45}$$
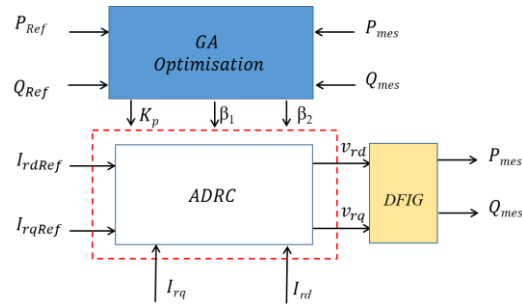
Figure 10. GA-based ADRC optimization

The best score value and mean score versus generation for the two control methods are represented in Figure 11. The parameters' evolution trought the generation is presented in Figure 12. The backstepping gains K_1 and K_2, and the ARDC controller parameters K_p, β_1 and β_2 are listed in Table 3.
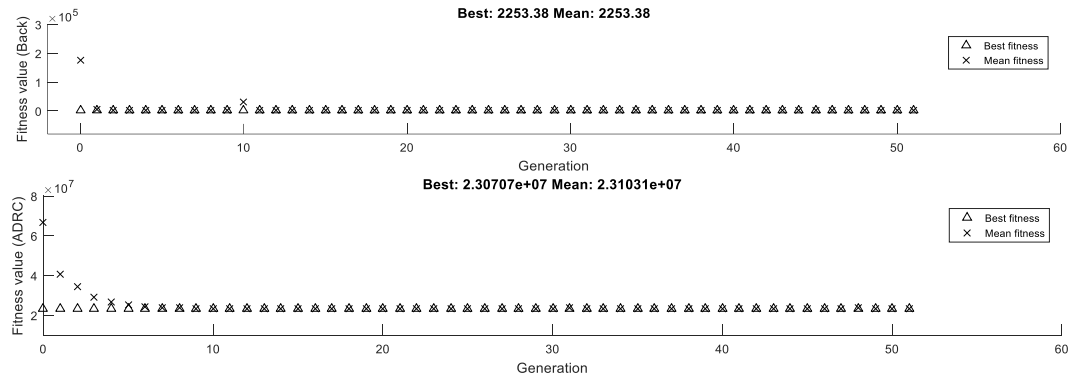

Figure 11. Backstepping and ADRC fitness value

Table 3. Backstepping and ADRC parameters' values

Parameter	Symbol	Value obtained by GA	Lower range	Upper range
Backstepping gain 1	K_1	38824	1.0	50000
Backstepping gain 2	K_2	29986	1.0	50000
Currents controller gain (ADRC)	K_p	17175	1.0	20000
Extended state observer gains (ADRC)	β_1	4357.5	1.0	5000
	β_2	481940	1.0	500000
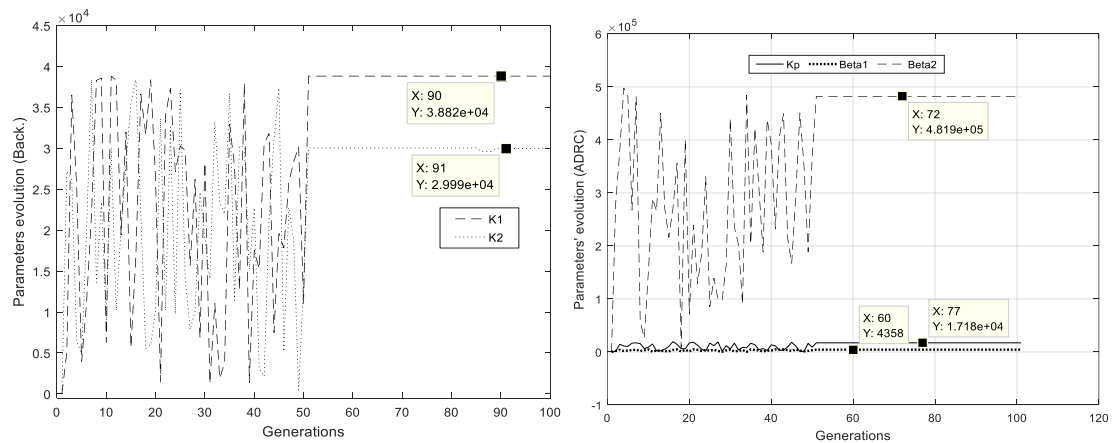
Figure 12. Parameters' evolution through the generation

3. RESULTS AND DISCUSSION
3.1. Tracking and control test

The parameters of the DFIG are listed in Table 4. In Figure 13 we represent the wind profile used in this work which is modelled by (46):

$$v(t) = 8 + 2\sin\left(2.5t - \frac{\pi}{5}\right) + 2\sin\left(4t - \frac{\pi}{3}\right) + 1.5\sin\left(5.4t - \frac{\pi}{12}\right) + 0.5\sin\left(2.5t - \frac{\pi}{12}\right) \qquad (46)$$

Figures 14 and 15 show the simulation results of the produced powers and the rotor currents I_{rd} and I_{rq} with their references, for the Backstepping technique and ADRC. The reference reactive power is chosen zero to guarantee a unit power factor. As can be seen in the previous figures, the produced powers controlled by backstepping and ADRC, optimized by genetic algorithm, follow perfectly their references. We can notice more precision and stability with a response without fluctuations or exhibiting overshoot on that based on the backstepping technique. From these figures, we can see that the stator currents vary according to the wind profile provided for the simulation and the frequency of the rotor voltages follows the DFIG speed variation. In Figure 16, we present the stator currents and rotor voltages of the DFIG.

Table 4. List of DFIG parameters

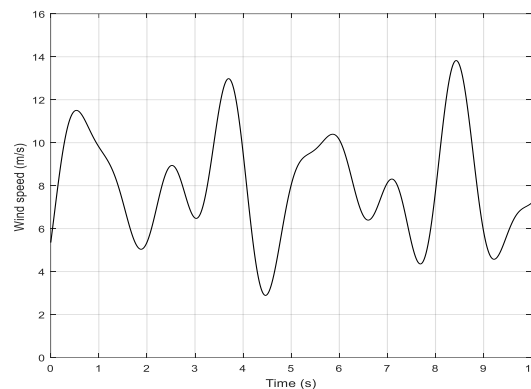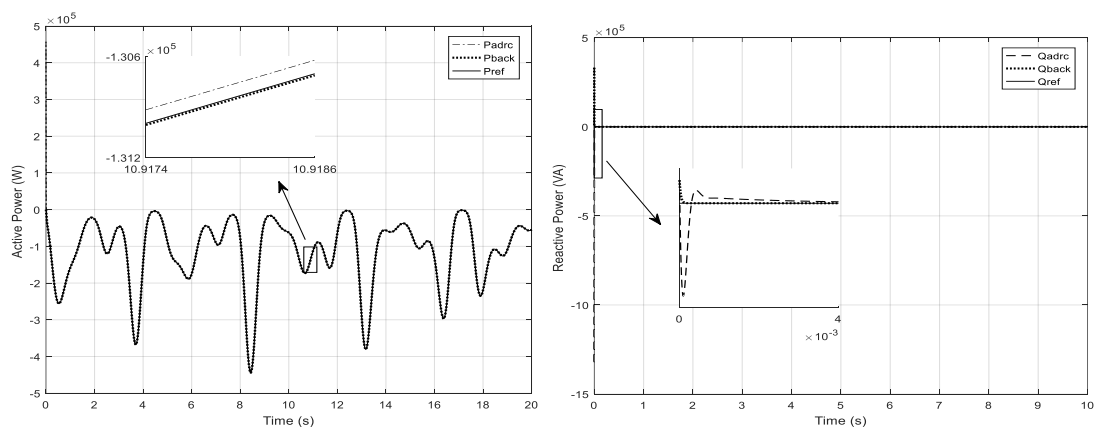| Parameter	Symbol	Value
Rated power	Ps	1.5 MW
Stator resistance	Rs	0.0089 Ω
Rotor resistance	Rr	0.0137 Ω
Stator inductance	L_s	0.0137 H
Rotor inductance	L_r	0.01367 H
Mutual cyclic inductance	L_m	0.0135 H
Number of pole pairs	p	2
Optimal tip speed ratio of turbine	λ_{opt}	8.1
Maximal power coefficient	C_{pmax}	0.48

Figure 13. The wind speed profile
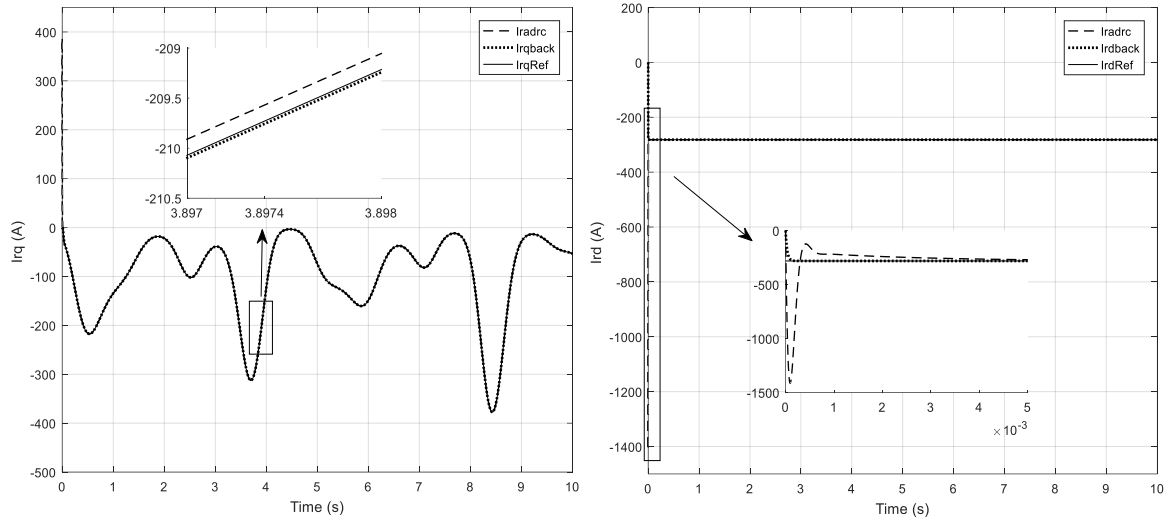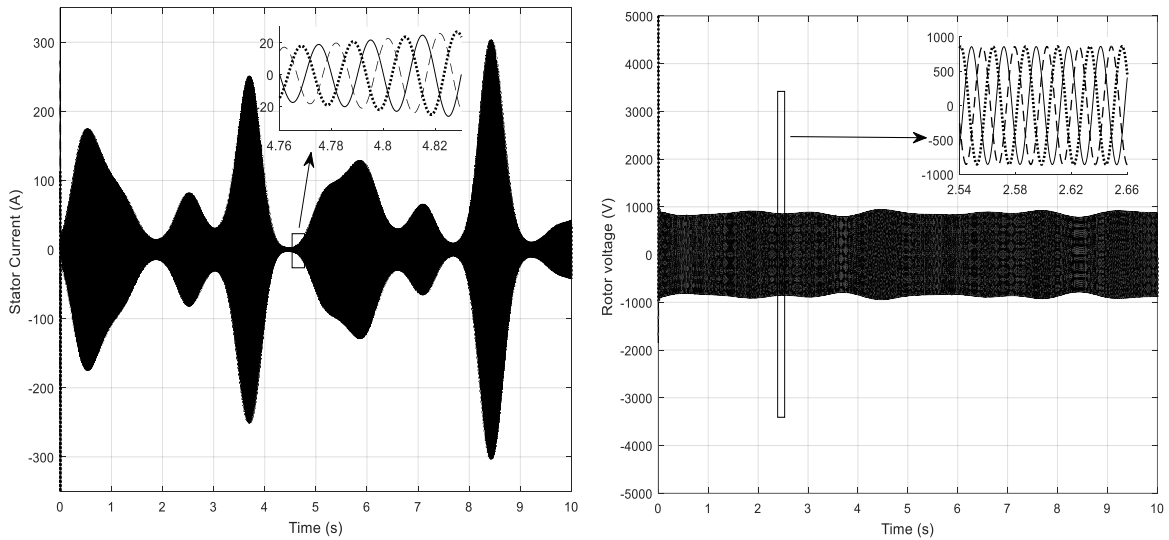

Figure 14. Active and reactive power

Figure 15. Rotor current I_{rq}, I_{rd} and its reference

Figure 16. Stator current and rotor voltage

3.2. Test of the robustness

The objective of the robustness test is to verify the control methods performance against the internal parameters variation of the DFIG. In fact, the regulator parameters computing is based on a DFIG model whose parameters are considered to be fixed. We are more particularly interested in highlighting the performance limits of the backstepping method in this case. However, these parameters can change over time or because of external phenomena. In Figures 17 and 18 we represent the produced powers evolution and the rotor currents I_{rq} and I_{rd} after a variation R_r and L_r with a rate of 100%.

From the Figures 17 and 18, the variations of the R_r and L_r values did not have much impact on the performance of the system controlled by the active disturbances rejection control unlike the backstepping technique. Indeed, the ADRC allows the estimation and compensation of disturbances. The tracking of the reference values is always assured as well as the stability which is not affected.
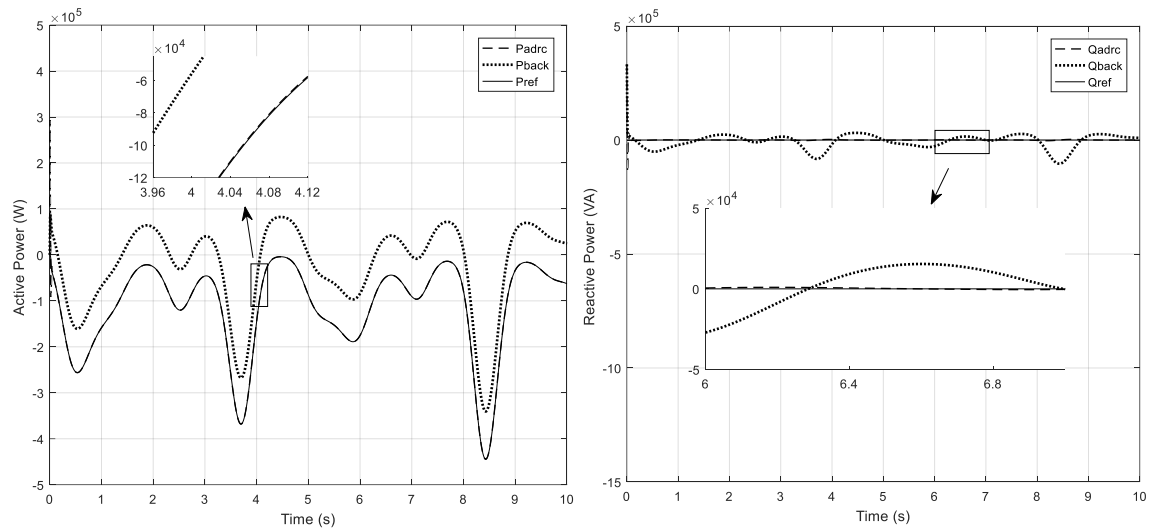
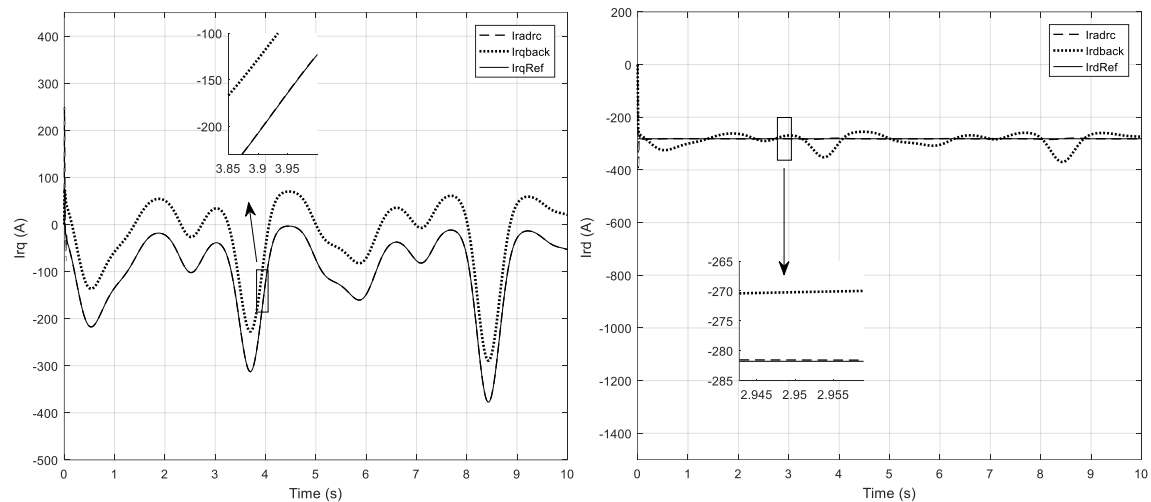Figure 17. Produced powers after a 100% variation of Rr and Lr

Figure 18. Currents I_{rq}, I_{rd} and its reference after a 100% variation of Rr and Lr

4. CONCLUSION

In this research article, we have dealt the modeling and control of the wind turbine driven by DFIG. We are interested to highlight and evaluate the dynamic performances of ADRC and backstepping methods and their sensitivity to the DFIG's internal parameters variation. The two control methods studied consist in controlling the rotor currents in order to adapt the DFIG rotation speed to the wind speed, by the control of the electromagnetic torque, and also in controlling the active and reactive powers injected into the grid. The synthesis of the regulation parameters is based on the genetic algorithm which allows to have the optimal values to guarantee the best performances. According to the simulation results, and for normal operation assuming that the DFIG's internal parameters are fixed, we notice that the backstepping control, optimized by GA, allows good performances, in particular a fast response and without overshoot, unlike the ADRC which has some undulations at the start. However, internal parameters are always subject to variations. In that case, we have found that the ADRC allows a good tracking of the desired values as well as a robustness against the DFIG's internal parameters variation. In terms of perspectives, the rate of the internal parameter's variation treated in this work is equal to 100%. However, we do not find any work that studies the order of magnitude of this variation rate, in order to have more precise values. We are therefore considering the development of methods or algorithms making it possible to estimate this variation rate and take it into account in the control laws used.

REFERENCES

[1] M. G. Molina and J. M. Alvarez, "Technical and Regulatory Exigencies for Grid Connection of Wind Generation," *Wind Farm–Technical Regulations, Potential Estimation and Siting Assessment, InTech*, June 2011, doi: 10.5772/16474.

[2] Y. Boussairi, A. Abouloifa, I. Lachkar, C. Aouadi, and A. Hamdoun, "State Feedback Nonlinear Control Strategy for Wind Turbine System Driven by Permanent Magnet Synchronous Generator for Maximum Power Extraction and Power Factor Correction," in *Vibration Analysis and Control in Mechanical Structures and Wind Energy Conversion Systems*. London, United Kingdom: IntechOpen, 2018, doi: 10.5772/intechopen.72366, [Online]. Available: https://www.intechopen.com/chapters/59835.

[3] S. Elaimani, "Modélisation de différentes technologies d'éoliennes intégrées dans un réseau de moyenne tension," Ph.D Thesis, University of science and technology in Lille, 2004.

[4] R. Rouabhi, "Contrôle des puissances générées par un système éolien à vitesse variable basé sur une machine asynchrone double alimentée," PhD Thesis, University of Batna, 2016.

[5] B. Hamane, M. L. Doumbia, M. Bouhamida, A. Draou, H. Chaoui, and M. Benghanem, "Comparative study of PI, RST, sliding mode and fuzzy supervisory controllers for DFIG based wind energy conversion system," *International Journal of Renewable Energy Resarch*, vol. 5, no. 4, pp. 1174–1185, 2015, doi: 10.20508/ijrer.v5i4.2915.g6705.

[6] Y. Djereri, "Commande directe du couple et des puissances d'une MADA associée à un système éolien par les techniques de l'intelligence artificielle," PhD Thesis, Djilali liabes University, 2015.

[7] O. Zamzoum, Y. El Mourabit, M. Errouha, A. Derouich, and A. El Ghzizal, "Power control of variable speed wind turbine based on doubly fed induction generator using indirect field-oriented control with fuzzy logic controllers for performance optimization," *Energy Science & Engineering*, vol. 6, no. 5, pp. 408-423, 2018, doi: 10.1002/ese3.215.

[8] H. Elaimani, A. Essadki, N. Elmouhi, and R. Chakib, "The Modified Sliding Mode Control of a Doubly Fed Induction Generator for Wind Energy Conversion During a Voltage Dip," *2019 International Conference on Wireless Technologies, Embedded and Intelligent Systems (WITS)*, 2019, pp. 1-6, doi: 10.1109/WITS.2019.8723712.

[9] H. Becheri, I. K. Bousarhanne, A. Harrouz, H. Glaoui, and T. Belbekri, "Maximum Power Point Tracking of Wind Turbine Conversion Chain Variable Speed Based on DFIG," *International Journal of Power Electronics and Drive System (IJPEDS)*, vol. 9, no. 2, pp. 527-535, June 2018, doi: 10.11591/ijpeds.v9.i2.pp527-535.

[10] M. Nadour, A. Essadki, and T. Nasser, "Comparative Analysis between PI & Backstepping Control Strategies of DFIG Driven by Wind Turbine," *International Journal of Renewable Energy Research (IJRER)*, vol. 7, no. 3, pp. 1307-1316, January 2017, doi: 10.20508/ijrer.v7i3.6066.g7163.

[11] B. Bossoufi, M. Karim, A. Lagrioui, M. Taoussi, and A. Derouich, "Observer backstepping control of DFIG-Generators for wind turbines variable-speed: FPGA-based implementation," *Renewable Energy*, vol. 81, pp. 903-917, September 2015, doi: 10.1016/j.renene.2015.04.013.

[12] A. G. Abo-Khalil, W. Alharbi, A.-R. Al-Qawasmi, M. Alobaid, and I. Alarifi, "Modeling and control of unbalanced and distorted grid voltage of grid-connected DFIG wind turbine," *International Transactions on Electrical Energy Systems*, vol. 31, no. 5, p. e12857, March 2021, doi: 10.1002/2050-7038.12857.

[13] R. Rouabhi, A. Rachid, C. Aissa, and D. E. Ali, "Hybrid Backstepping Control of a Doubly Fed Wind Energy Induction Generator," *The Mediterranean Journal of Measurement and Control*, vol. 11 no. 1, pp. 367-376, 2015.

[14] C. Hamid, *et al.*, "Performance improvement of the variable speed wind turbine driving a DFIG using nonlinear control strategies," *International Journal of Power Electronics and Drive Systems (IJPEDS)*, vol. 12, no. 4, pp. 2470-2482, December 2021, doi: 10.11591/ijpeds.v12.i4.pp2470-2482.

[15] A. Radaideh, M. Bodoor, and A. Al-Quraan, "Active and Reactive Power Control for Wind Turbines Based DFIG Using LQR Controller with Optimal Gain-Scheduling," *Journal of Electrical and Computer Engineering*, 2021, doi: 10.1155/2021/1218236.

[16] K. E. Okedu, M. A. Tobi, and S. A. Araimi, "Comparative Study of the Effects of Machine Parameters on DFIG and PMSG Variable Speed Wind Turbines During Grid Fault," *Frontiers in Energy Research*, vol. 9, p. 174, May 2021, doi: 10.3389/fenrg.2021.681443.

[17] A. Lazrak and A. Abbou, "An Improved Control Strategy for DFIG Wind Turbine to Ride-Through Voltage Dips," *2018 6th International Renewable and Sustainable Energy Conference (IRSEC)*, 2018, pp. 1-6, doi: 10.1109/IRSEC.2018.8703017.

[18] M. S. El-Moursi, B. Bak-Jensen and M. H. Abdel-Rahman, "Novel STATCOM Controller for Mitigating SSR and Damping Power System Oscillations in a Series Compensated Wind Park," *in IEEE Transactions on Power Electronics*, vol. 25, no. 2, pp. 429-441, February 2010, doi: 10.1109/TPEL.2009.2026650.

[19] S. El Aimani, "Practical identification of a DFIG based wind generator model for grid assessment," *2009 International Conference on Multimedia Computing and Systems*, 2009, pp. 278-285, doi: 10.1109/MMCS.2009.5256686.

[20] J. Lopez, E. Gubia, E. Olea, J. Ruiz, and L. Marroyo, "Ride Through of Wind Turbines with Doubly Fed Induction Generator Under Symmetrical Voltage Dips," *IEEE Transactions on Industrial Electronics*, vol. 56, no. 10, pp. 4246-4254, October 2009, doi: 10.1109/TIE.2009.2028447.

[21] N. Elmouhi, A. Essadki, H. Elaimani, and R. Chakib, "Evaluation of the Inertial Response of Variable Speed Wind Turbines Based on DFIG using Backstepping for a Frequency Control," *2019 International Conference on Wireless Technologies, Embedded and Intelligent Systems (WITS)*, 2019, pp. 1-6, doi: 10.1109/WITS.2019.8723766.

[22] M. Nadour, A. Essadki, T. Nasser, and M. Fdaili, "Robust coordinated control using backstepping of flywheel energy storage system and DFIG for power smoothing in wind power plants," *International Journal of Power Electronics and Drive System (IJPEDS)*, vol. 10, no. 2, pp. 1110-1122, June 2019, doi: 10.11591/ijpeds.v10.i2.pp1110-1122.

[23] M. El Azzaoui, H. Mahmoudi, and K. Boudaraia, "Backstepping Control of Wind and Photovoltaic Hybrid Renewable Energy System," *International Journal of Power Electronics and Drive Systems (IJPEDS)*, vol. 7, no. 3, pp. 677–686, September 2016, doi: 10.11591/ijpeds.v7.i3.pp677-687.

[24] C. Yang, X. Yang, and Y. A. W. Shardt, "An ADRC-based control strategy for FRT improvement of wind power generation with a doubly-fed induction generator," *Energies*, vol. 11, no. 5, p.1150, 2018, doi: 10.3390/en11051150.

[25] M. Saleem, B.-S. Ko, S.-H. Kim, S. Kim, B. S. Chowdhry, and R. Y. Kim, "Active Disturbance Rejection Control Scheme for Reducing Mutual Current and Harmonics in Multi-Parallel Grid-Connected Inverters," *Energies*, vol. 12, no. 22, p. 4363, 2019, doi: 10.3390/en12224363.

[26] M. Penne, W. Qiao, L. Qu, L. Qu, R. Huang, and Q. Huang, "Active Disturbance Rejection Control of Doubly-Fed Induction Generators Driven by Wind Turbines," *2021 IEEE Energy Conversion Congress and Exposition (ECCE)*, 2021, pp. 965-972, doi: 10.1109/ECCE47101.2021.9595083.

[27] A. Boukhriss, T. Nasser, A. Essadki, and A. Boualouch, "Active Disturbance Rejection Control for DFIG Based Wind Farms Under Unbalanced Grid Voltage," *International Review on Modelling and Simulations (IREMOS)*, vol. 7, no. 1, pp. 95-105, 2014, doi: 10.15866/iremos.v7i1.265.

[28] E. M. Boulaoutaq, M. Kourchi, and A. Rachdy, "Nonlinear ADRC Applied on Wind Turbine Based on DFIG Operating at its Partial Load," *2019 International Conference of Computer Science and Renewable Energies (ICCSRE)*, 2019, pp. 1-8, doi: 10.1109/ICCSRE.2019.8807773.

[29] A. Boulmane, Y. Zidani, D. Belkhayat, and M. Bouchouirbat, "A GA-based adaptive mechanism for sensorless vector control of induction motor drives for urban electric vehicles, "*Turkish Journal of Electrical Engineering and Computer Sciences*, vol. 28, no. 3, pp. 1731–1746, 2020, doi: 10.3906/elk-1910-39.

[30] Ö. Aydoğdu and R. Akkaya, "An effective real coded GA based fuzzy controller for speed control of a BLDC motor without speed sensor," *Turkish Journal of Electrical Engineering & Computer Sciences*, vol. 19, no. 3, pp. 413-430, 2011, doi: 10.3906/elk-0907-122.

[31] R. Arulmozhiyal and K. Baskaran, "Speed Control of Induction Motor using Fuzzy PI and Optimized using GA," *International Journal of Recent Trends in Engineering*, vol. 2, no. 5, pp. 43-47, November 2009.

[32] A. Guediri, A. Guediri, and S. Touil, "Optimization Using a Genetic Algorithm Based on DFIG Power Supply for the Electrical Grid," *International Journal of Engineering*, vol. 35, no. 01, pp. 121-129, January 2022, doi: 10.5829/IJE.2022.35.01A.11.

[33] C. Ahmed, A. Bekri, H. Gouabi, and H. Ali, "Non-linear backstepping control optimized by genetic algorithm for the control of a wind turbine," *International Journal of Industrial Electronics and Electrical Engineering*, vol. 7, no. 6, pp. 3–7, June 2019.

BIOGRAPHIES OF AUTHORS

Noureddine Elmouhi 🆔 🔍 SC Ⓟ was born in Marrakesh, Morocco in 1987. He received the the Engineer Degree in Electrical Engineering, from sciences and technologies Faculty (FST), Marrakesh, Morocco, in 2010. He is currently preparing a Ph.D thesis in Research Center of Engineering and Health Sciences and Technologies (STIS), Ecole Nationnale Supérieure d'Arts et Métiers (ENSAM), Mohammed V University in Rabat, Morocco. He can be contacted at email: n.elmouhi@gmail.com.

Ahmed Essadki 🆔 🔍 SC Ⓟ is currently a professor and university research professor at the electrical engineering department of ENSAM, Mohammed V University Morocco**.** In 2000, he received his Ph.D degree from Mohammedia Engineering School (EMI), Morocco. From 1990 to 1993, he pursued his master program at UQTR university, Quebec Canada, respectively, all in electrical engineering. His current research interests include renewable energy, motor drives and power system. Essadki is a member of RGE Lab in research group leader. He can be contacted at email: ahmed.essadki1@gmail.com.

Hind Elaimani 🆔 🔍 SC Ⓟ was born in Marrakesh, Morocco in 1988. She received the Master Degree in Electrical Engineering, from sciences and technologies Faculty (FST), Marrakesh, Morocco, in 2011. She is currently preparing a Ph.D thesis in Research Center of Engineering and Health Sciences and Technologies (STIS), Ecole Nationnale Supérieure d'Arts et Métiers (ENSAM), Mohammed V University in Rabat, Morocco. She can be contacted at email: h.elaimani@gmail.com.